Macromol. Symp. **2004**, *205*, 71—84

Characterization of Polypropylene (PP) Nanocomposites for Industrial Applications

Athina Korakianiti,[1] *Vasiliki Papaefthimiou,*[1,2] *Theofania Daflou,*[1,2] *Stella Kennou,*[1,2] *Vasilis G. Gregoriou**[1]

[1] Foundation for Research and Technology-Hellas, Institute of Chemical Engineering and High Temperature Processes (FORTH - ICE/HT), Patras 26504, Greece
[2] Department of Chemical Engineering, University of Patras, Patras, 26500, Greece
E-mail: gregoriou@iceht.forth.gr

Summary: This study aims in the examination of a new class of materials named polymer layered silicate nanocomposites. In our case, composites are usually combinations of polypropylene matrix with solid mineral reinforcements named silicates (e,g. montmorillonite, a natural clay). In this study, two complementary techniques used to characterize nanocomposites. Fourier transform infrared spectroscopy (FT-IR) both in transmission and attenuated total reflectance (ATR) modes combined with X-ray photoelectron spectroscopy (XPS).

Keywords: nanofillers; polypropylene nanocomposites; spectroscopy

Introduction

Nanocomposites are a new class of materials that are particle filled-polymers for which at least one dimension of the dispersed particles is in nanometer range. In the case of plastics, nanocomposites are usually combinations of polymer matrix with solid mineral reinforcements. They can have favorable properties, like high stiffness and barrier resistance. Polypropylene (PP) is one of the most widely used polyolefins polymers for many applications due to its low cost, low density, high thermal stability and resistance to corrosion. It is also a polymorphic material with three known possible crystalline phases namely a) monoclinic, b) hexagonal and c) triclinic. [1] Since it does not include any polar groups in its backbone, it was thought that the homogeneous dispersion of the silicate layers in PP would not be realized. [2] Blending polypropylene with clays to form nanocomposites is a way to increase its utility by improving its

DOI: 10.1002/masy.200450107

mechanical properties. The nanoclays used are the products of the reaction of montmorillonite with coupling agents named also alchoxysilanes. The layered silicates commonly used belong to the structural family known as the 2:1 phyllosilicates. Their crystal lattice consists of two-dimensional layers. These layers organize themselves to form stacks with a regular van der Walls gap in between them called *interlayer* or *gallery*. Polymer layered-silicate (PLS) nanocomposites have maximized polymer-clay interactions since the clay is dispersed on a nanometer scale. The best properties are obtained if the clay is fully exfoliated into single clay layers. [3]

The purpose of this study is the spectroscopic characterization and evaluation of a variety of materials based on thermoplastic matrices and reinforced with inorganic nanofillers that can be used for industrial applications. Furthermore, we try to verify whether and how nanofillers can enhance mechanical and thermal properties in order to produce lighter manufactured parts for industrial applications.

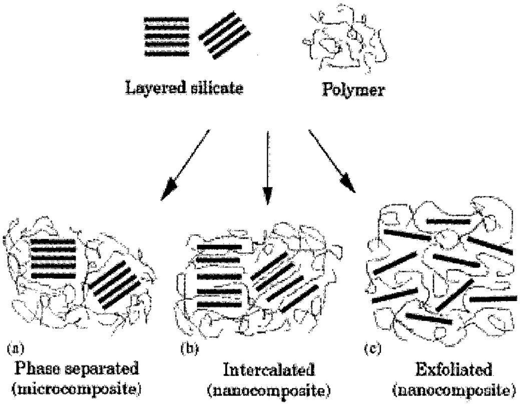

Figure 1: Depending on the nature of the components used (layered silicate, organic cation and polymer matrix) and the method of preparation, three main types of composites may be obtained when layered clay is associated with a polymer. [4]

Figure 1 shows that beyond the conventional phase separated polymer/silicate composites, for which the polymer and the inorganic host remain immiscible, two extra types of hybrids are possible. *Intercalated* in which extended polymer chains are sandwiched in between silicate layers, and *exfoliated*, where the separated, individual silicate layers are more or less uniformly dispersed in the polymer matrix.

Recently, maleic anhydride (MA) was used to make a kind of in situ compatibilizer which acted at the interface to reduce the interfacial tension between the matrix and the dispersed thermotropic liquid crystalline phase. It was observed that maleic anhydride-PP partly acts as a nucleating agent for the matrix. Also, the presence of MA-PP in the iPP was said to affect the crystallization of iPP by acting as a nucleating agent. [5]

In this study, FT-IR both in transmission and ATR mode is used in conjunction with XPS to analyze the structure of intercalated silicates. It is said that the interactions of polymers with interfaces, which substantially modify the solid-liquid or liquid-air interface in many important industrial and natural processes, can also be monitoring using FT-IR. [6] FT-IR spectroscopy complements other techniques in providing detailed information on the chain conformation transition and crystallinity of a polymer with nondestructive and fast feature. Furthermore, XPS is a powerful tool for the investigation of the surface chemistry in such systems.

Experimental Section

The materials used in the present study were Cloisite 20 A (purchased by Southern Clay Products), Polybond 3100 and 3200 -which is made up of maleic anhydride homopolymer polypropylene- (purchased by Uniroyal Chemical Co.Inc) and PP-M (isotactic polypropylene purchased by BASF). Prof. Dan Donescu, Institute of Chemical Research, 77208-Bucharest, Romania, provided nanocomposites and all modified clays. Furthermore, Cloisites 15A and 20A are natural montmorillonite modified with a quaternary ammonium salt. They have the same organic modifier but the only difference between them is their concentration. Cloisite 20A is characterized by a moderate negative surface charge of 95 meq /100g clay whereas Cloisite 15A of 125 meq /100g clay.

Table 1: List of nanofillers used

MPTS 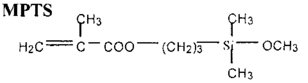 $H_2C{=}\overset{CH_3}{C}{-}COO{-}(CH_2)_3{-}\underset{CH_3}{\overset{CH_3}{Si}}{-}OCH_3$	**TMES** 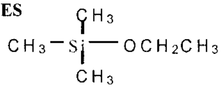 $CH_3{-}\underset{CH_3}{\overset{CH_3}{Si}}{-}OCH_2CH_3$	**OTES** 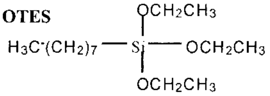 $H_3C(CH_2)_7{-}\underset{OCH_2CH_3}{\overset{OCH_2CH_3}{Si}}{-}OCH_2CH_3$
HSTMS 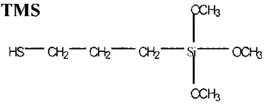 $HS{-}CH_2{-}CH_2{-}CH_2{-}\underset{OCH_3}{\overset{OCH_3}{Si}}{-}OCH_3$	**MeTES** 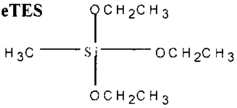 $H_3C{-}\underset{OCH_2CH_3}{\overset{OCH_2CH_3}{Si}}{-}OCH_2CH_3$	**PTES** 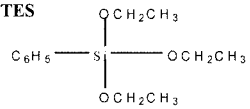 $C_6H_5{-}\underset{OCH_2CH_3}{\overset{OCH_2CH_3}{Si}}{-}OCH_2CH_3$
GMPS 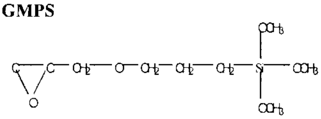	**TEOS** 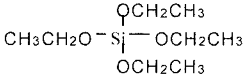 $CH_3CH_2O{-}\underset{OCH_2CH_3}{\overset{OCH_2CH_3}{Si}}{-}OCH_2CH_3$	**VTES** 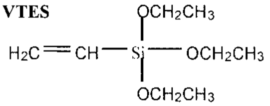 $H_2C{=}CH{-}\underset{OCH_2CH_3}{\overset{OCH_2CH_3}{Si}}{-}OCH_2CH_3$

Table 2: List of samples used

PP-3150	PP, 14,3 % Polybond 3150
PP-3200	PP, 14,3 % Polybond 3200
PP-D1R	PP, 14,3 % Polybond 3150 and 6,1 % Cloisite 20A
PP-D2R	PP, 14,3 % Polybond 3200 and 6,1 % Cloisite 20A
PP-D6R	PP, 14,3 % Polybond 3200 and 6,1 % Cloisite 20A modified with MPTS
PP-D8R	PP, 14,3 % Polybond 3200 and 6,1 % Cloisite 20A modified with OTES
PP-D9	PP, 6,1 % Cloisite 20 A modified with MPTS
PP-D10	PP, 6,1 % Cloisite 20A modified with OTES

Two complementary techniques used to characterize nanocomposites. Fourier Transform Infrared Spectroscopy (FT-IR) both in transmission and attenuated total reflectance (ATR) modes with X-ray Photoelectron Spectroscopy (XPS) took place in order to analyze nanocomposites materials. Firstly, Attenuated Total Reflectance (ATR) FT-IR Spectroscopy was performed using a Nicolet 20DXB spectrometer. A zinc selenide (ZnSe) crystal was used as the internal reflection element. The spectrometer is equipped with a Mercury Cadmium Telluride (MCT) detector. The infrared transmission spectra were recorded using a Nicolet 850 FT-IR spectrometer equipped with a DTGS-KBr detector. Each measurement was the accumulation of scans at 4 cm^{-1} spectral resolution. The number of scans was 1024. Secondly, XPS technique was carried out in a commercial ultrahigh vacuum system, which consists of a fast entry specimen assembly, a preparation and an analysis chamber. The analysis chamber is equipped with a hemispherical electron energy analyzer (SPECS LH-10), a twin anode X-ray gun for XPS and a discharge lamp for UPS measurements. The base pressure was 5×10-10 mbar. All spectra were taken at normal emission. The spectrometer was calibrated using the Fermi edge position of a sputter-cleaned Au foil, which was defined as Binding Energy (BE) zero of the spectra. Unmonochromatized AlKα line at 1486.6 eV and analyzer pass energy of 97 eV, giving a Full Width at Half Maximum (FWHM) of 1.8 eV for the Au $4f_{7/2}$ peak of a clean Au foil, were used in all XPS measurements. The electron binding energies were referenced to the $Au4f_{7/2}$ peak of the Au foil, at 84.00±0.05 eV. The XPS core level spectra were analyzed with a fitting routine which decomposes each spectrum into individual, mixed Gaussian-Lorentzian peaks using a Shirley background subtraction over the energy range of the fit. The nanopowders were mounted in the sample holder in the form of pellets while the polypropylene nanocomposites were simply placed on it. The pressure was increasing (up to $\sim 10^{-8}$ mbar) during the sample exposure to X-rays in all cases. Before introducing the nanopowders in the UHV, they were heated up to 100° C for several weeks in order to remove humidity.

Results and Discussion

The Cloisite 20A XPS survey spectrum shows that the surface of Cloisite 20A (without modification with the coupling agents) consists of Carbon, Oxygen, Silicon and Aluminum. Figure 2 shows the C1s, O1s, Si2p and Al2p XPS spectra of Cloisite 20A. The XPS C1s peak (fig. 2a) was analyzed into three components, at binding energies 285 eV, 286.5 eV and 287.5±0.05 eV, which correspond to C-H, C-O-C or C-OH and C=O groups respectively. The XPS O1s peak (fig. 2b) was analyzed into three components, at binding energies 532.2±0.05 eV (C=O), 533±0.05 eV (C-O-C or C-OH) and 535±0.05 eV (H_2O). The XPS Si 2p peak (fig. 2c) was analyzed into three components, at binding energies 100±0.05 eV (Si^0), 102 eV (SiO_x) and 104 eV (SiO_2). The Al2p peak (fig. 2d) was analyzed in two components at binding energies 74.7 and 76.7±0.05 eV, which correspond to Al_2O_3 and Al_2O_x respectively.

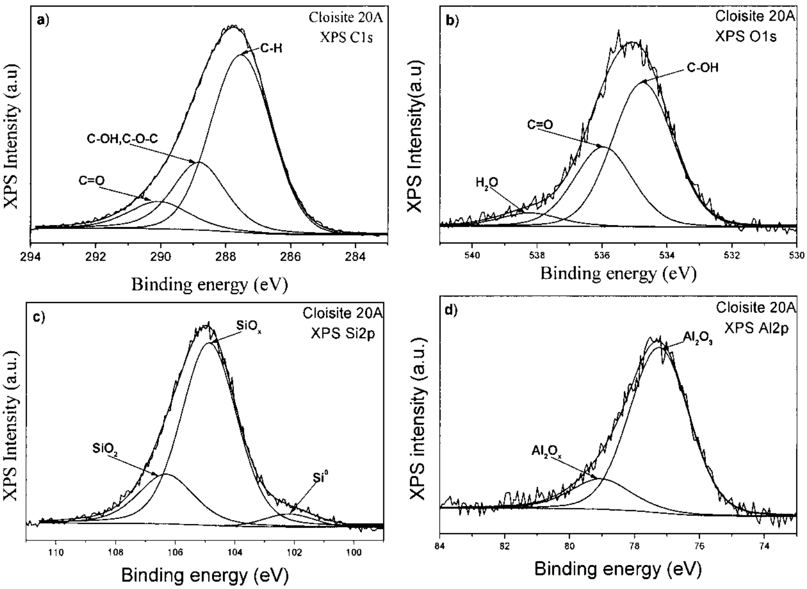

Figure 2: C1s, O1s, Si2p and Al2p XP-spectra of Cloisite 20 A.

On the other hand, FT-IR measurements provide direct information on the structure of the interlayer as well as the method to relate the intercalated state to the corresponding bulk state. [7]

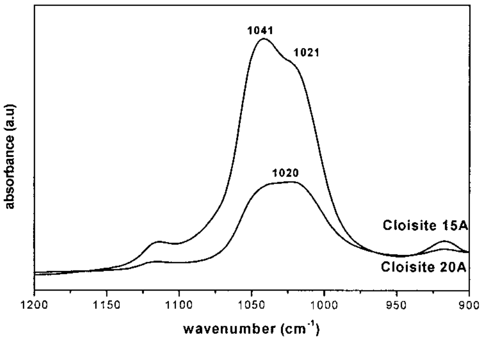

Figure 3: FT-IR spectra of Cloisite 15A and Cloisite 20A and the differences for the Si-O-C stretching vibrations.

Figure 3 compares the two different Cloisites used 15A to 20A. The FT-IR spectrum of these samples implies that the characteristic intense band at 1110-1000 cm^{-1} assigned to the asymmetric Si-O-C stretching vibration show differences for the different Cloisites studied, most likely attributed to the different levels of hydration in the samples.

Furthermore, quantitative XPS analysis of Cloisite 20A and Cloisite 15A showed that the percentage of silicon in Cloisite 20A was increased by 120% regarding Cloisite 15A, while the percentage of aluminium is decreased by 50% regarding Cloisite 15A.

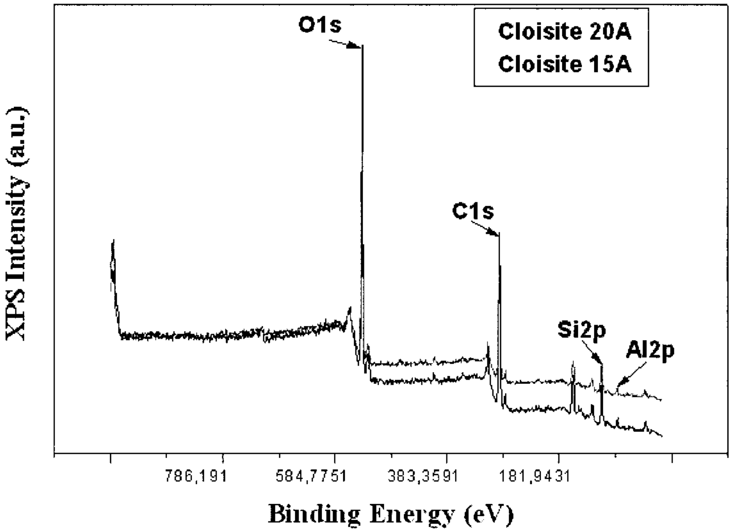

Figure 4: Comparative spectrum of different Cloisites used.

Figure 4 shows the XPS wide scans of Cloisite 20A and Cloisite 15A, respectively.

Also, there were examined the nanoscaled clays which are the products of montmorillonite (MMT) with coupling agents.

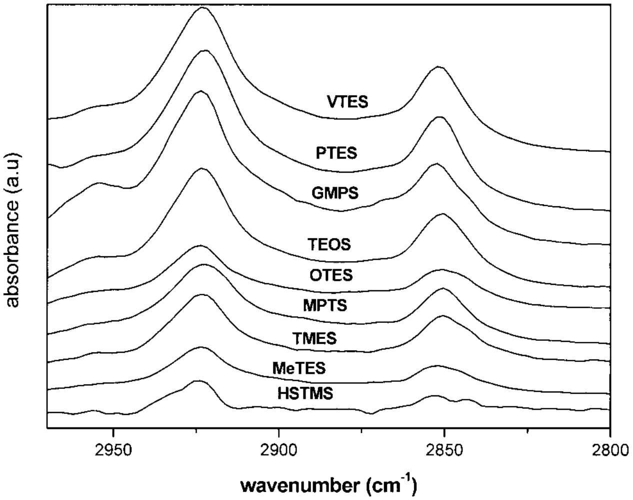

Figure 5: The frequency shifts of the CH_2 stretching vibrations relates to the interlayer packing density.

Figure 5 is indicative of the interaction between the alchoxysilanes and Cloisite 20A. We have monitored the frequency shift of the asymmetric CH_2 stretching vibrations as a function of interlayer packing density. There are similarities in the OTES and TMES at 2923 cm^{-1}, MPTS, GMPS and PTES appear to have the same band at 2922 cm^{-1}, MeTES at 2923cm^{-1}, VTES have a peak at 2923 cm^{-1} and finally HSTMS has the same band as Cloisite 20A at 2923 cm^{-1}. Also, at 2822 cm^{-1} HSTMS, MeTES and TEOS appear the same peak as Cloisite 20A, whereas the rest have common peaks at 2850 cm^{-1}, apart from a shift at 2852 cm^{-1} in GMPS and PTES samples. Table 3 presents the above assignments.

Table 3: The strongest aliphatic absorption bands observed of the methylene modes in between 3000-2800 cm^{-1}

Sample	Wavenumber (cm^{-1})
OTES, TMES, VTES, HSTMS	2850, 2923
MPTS	2850, 2922
MeTES	2850, 2922
PTES	2852, 2923
Cloisite 20A	2852, 2923
GMPS	2852, 2922

Shifts in that region reflect changes in chain conformation. Shifting from lower frequencies for ordered, all trans chains, to higher frequencies as chain disorder (gauche/trans conformer ratio) increases. [7]

Vaia et al [7], found that the intercalated chains exist in states with varying degrees or order by monitoring frequency shifts of the asymmetric CH_2 stretching and bending vibrations. When the available surface area per molecule is within a certain range, the chains are not completely disordered but retain some orientational order similar to that in the liquid crystalline state. As the interlayer packing density or the chain length decreases, the intercalated chains adopt amore disordered, liquid-like structure resulting from an increase in the gauche/trans conformer ratio. [5]

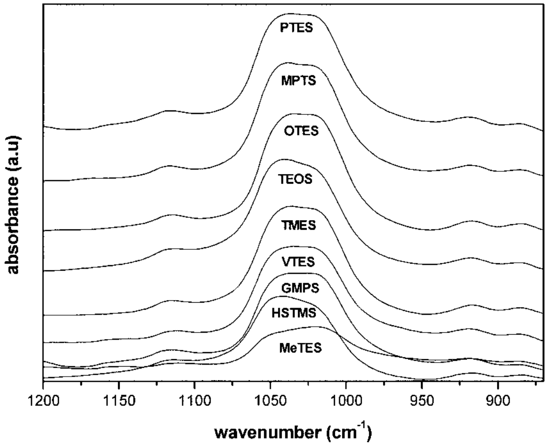

Figure 6: FT-IR spectra of MMT with coupling agents at the Si-O-C vibration region.

Figure 6 shows the fact that some peaks appear as double and other as single. These differences noticed in the relative intensity of the double peak in the 1100-1000 cm^{-1} region, are assigned to the asymmetric Si-O-C stretching vibration. In particular, MeTES have a peak at 1019 cm^{-1}, HSTMS and TEOS show a shift at 1041cm^{-1}, whereas the rest have double peaks, at about 1036 and 1022 cm^{-1}, respectively.

The XPS spectra (not shown) of the Cloisite 20A upon modification with the coupling agents depicted in table 1, were also recorded. Quantitative XPS analysis showed that the insertion of the coupling agents induced changes at the % concentration of the components of the modified Cloisite 20A, which were in good correlation with the hydrocarbon radicals of the silanes added. The O1s peak component at 533 eV increased by ~5 % by the insertion of the coupling agents, due to the contribution of their C-O-C (or C-OH) groups. Furthermore, an extra Al2p component appeared at the modified Cloisite 20 A with PTES at binding energy 71.5 eV, which corresponds to Al^0. On the whole, the changes observed at the XPS results of the modified Cloisite 20A samples confirm the presence of the silanes on the clay surface, but there is no chemical interaction observed.

Polypropylene nanocomposites were analyzed so as to examine if the addition of the clay changes the crystallinity of iPP, as it is said that the silicate layers acted as nucleating agents for crystallization of polypropylene. [8]

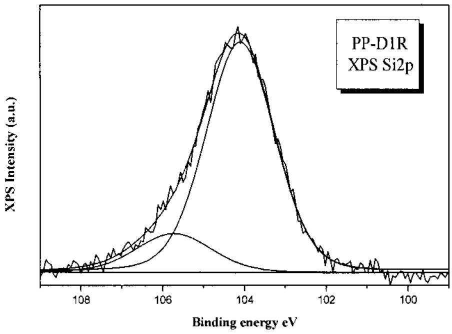

Figure 7: XPS C1s peak of PP-D1R

Figure 7 shows the XPS C1s peak of PP-D1R, which was analyzed into two components at binding energies 285±0.05 eV (C-H) and 286.5±0.05 eV (C-OH or C-O-C). In all cases XPS results showed that upon insertion of polybond and Cloisite 20A -or Cloisite 20A modified with coupling agents- in the PP-M matrix, the C1s component attributed to the –C=O bond disappears.

Moreover, in the infrared spectra of polypropylene nanocomposites, any difference in the bands in figure 5 can be used to indicate if an induced crystallinity took place or moreover to estimate the degree of crystallinity observed.

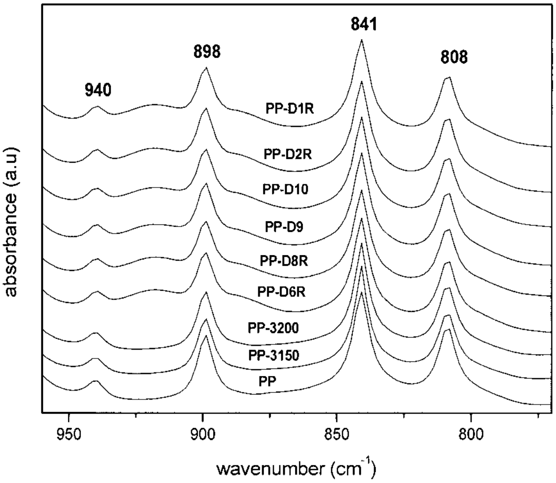

Figure 8: The FT-IR spectra of all the polypropylene nanocomposites modified with nanoclays.

Figure 8 shows that there is not any shift in the specific bands attributed to the isotactic PP. That can be a serious indication that crystallization of the polypropylene doesn't occur. So, nanoclays or maleic anhydrides do not change the physical mode of the polymer. The curves at about 889 and 918 cm^{-1} are assigned to the Cloisite 20A. Also, the band observed at 808 cm^{-1} is attributed to the rocking vibration of CH_2 and vC-CH_3. The band at 841 cm^{-1} is attributed to rocking CH_2, rocking CH_3 and vC-CH_3. The band that appears at 898 cm^{-1} is assigned to the rocking CH_3, rocking CH_2, bending CH. Since, there is no shift observed in the above spectra or the appearance of a new band, we can easily infer that no change in crystallinity is appeared caused by the presence of maleic anhydride in the iPP matrix. The several bands at 800-1200 cm^{-1} range that appear are attributed to the 3_1 helix, which is the regular conformation in all iPP polymorphs. The 841 cm^{-1} helix band is a commonly used one. [9]

Based on XPS analysis we notice that the PP-M survey spectrum shows that there is Carbon, Oxygen and Silicon at the surface of PP-M. Figure 9 shows the C1s, O1s and Si2p XPS spectra of PP-M. The existence of silicon is attributed to contamination during PP-M film preparation.

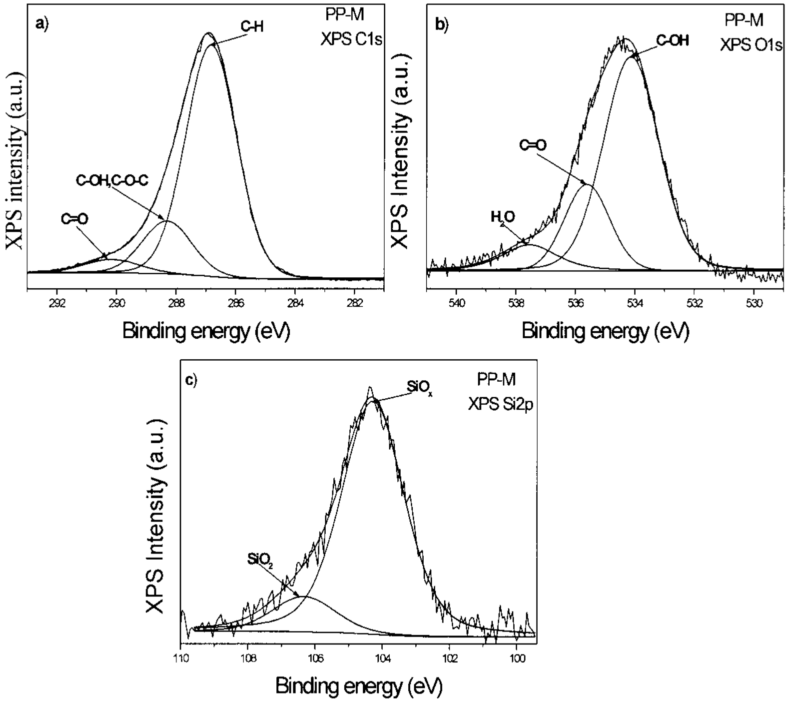

Figure 9: C1s, O1s and Si2p XP-spectra of PP-M.

Figure 9 shows the C1s, O1s and Si2p XPS spectra of PP-M. The XPS C1s peak (fig. 3a) was analyzed into three components, at binding energies 285 eV, 286.5 eV and 287.5±0.05 eV, which correspond to C-H, C-O-C (or C- OH) and C=O groups respectively. The XPS O1s peak (fig. 3b) was analyzed into three components, at binding energies 532.2±0.05 eV (C=O), 533±0.05 eV (C-O) and 535±0.05 eV (H_2O). The XPS Si 2p peak (fig. 3c) was analyzed into two components, at binding energies 102 eV (SiO_x) and 104 eV (SiO_2). The existence of the -C=O and C-OH or C-

O-C bonds in PP-M is due to the absorption of oxygen in the polymer matrix when it is exposed to the atmosphere [10]

Conclusions

FT-IR measurements provide for the first time direct information on the structure of the interlayer as well as the method to relate the intercalated state to the corresponding bulk state. The modifiers (HSTMS, VTES, TMES, OTES, MPTS, MeTES) and Cloisite 20A due to their low frequency have an ordered all-trans structure compared to the rest modifiers which show higher frequencies. Therefore, this fact can be considered an indication of the increase of the interlayer packing density for those modifiers. Also, the presence of the alkoxysilanes on the surface of Cloisite 20A is evident by the XPS results. Finally, the addition of maleic anhydride and Cloisite 20A does not change the crystallinity of the polymeric matrix therefore, no change in crystallinity was observed in the PP nanocompoistes.

Acknowledgments

The authors would like to thank Prof. Dan Donescu from Institute of Chemical Research in Bucharest, Romania for providing materials and information. This work was financial supported by E.U GROWTH Programme "PRONACOM". (No G5RD- CT2002-00721)

[1] J. X. Li and W. L. Cheung, *Polymer* **1998**, *39*, Number 26, 6935-6940.
[2] Masaya Kawasumi, Naoki Hasegawa, Makoto Kato, Arimitsu Usaki, and Akane Okada, *Macromolecules* **1997**, *30*, 6333-6338.
[3] E. P. Giannelis, R. Krishnamoorti, E. Manias, *Advances in Polymer Science* **1999**, Vol. *138*, 107-147.
[4] Michael Alexandre, Philippe Dubois, *Materials Science and Engineering*, **2001**, *28*, 1-63, *Reports: A Review Journal.*
[5] Yongsok Seo, Jinho Kim, Kwang Ung Kim, Young Chul Kim, *Polymer* **2000**, *41*, 2639-2646.
[6] David R. Scheuing, *Fourier Transform Infrared Spectroscopy in Colloid and Interface Science*, An Overview, *American Chemical Society* **1991**, Chapter 1, pages 1-21.
[7] Richard A. Vaia, Rachael K. Teukolsky, and Emmanuel P. Giannelis, *Chem. Mater.* **1994**, *6*, 1017-1022.
[8] Xiaohui Liu, Qiuju Wu, *Polymer* **2001**, 42, 10013-10019.
[9] Andreassen Erik, *Infrared and Raman spectroscopy of polypropylene*, *Kluwer Publishers* **1999**, 320-328.
[10] A. Rjeb, S. Letarte, L. Tajounte, Journal of Electron Spectroscopy and Related Phenomena **2000**, 107, 221-230.